Isabelle L. Arnaud
Jacques Josserand
Henrik Jensen*
Niels Lion
Christophe Roussel
Hubert H. Girault

Laboratoire d'Electrochimie Physique et Analytique,
Ecole Polytechnique Fédérale de Lausanne,
Lausanne, Switzerland

Salt removal during Off-Gel™ electrophoresis of protein samples

The Off-Gel™ technology was recently described for protein fractionation in a solution placed on top of an immobilized pH gradient gel. In addition, this process was found to remove salts from the biological samples to analyze. This desalting effect is studied experimentally in a conductometric prototype cell. A simplified analytical model is developed to understand this process and a good agreement is found with the conductivity measurements. To illustrate the desalting of a biological sample, a 1 $mg \cdot mL^{-1}$ solution of β-lactoglobulin A in 0.1 M NaCl is subjected to electrophoresis in a single compartment Off-Gel™ cell. The analysis of the resulting sample by ESI-MS demonstrates the effective removal of salt. A finite element diffusion-migration model is also used to illustrate how the nonuniformity of the electric field in the cell, associated with the salt migration, can slow down the desalting process.

Keywords: Conductivity / Finite element simulation / Off-Gel™ electrophoresis / Protein desalting
DOI 10.1002/elps.200410294

1 Introduction

Since its introduction in 1975, two-dimensional gel electrophoresis (2-DE) has been the method of choice for the separation and classification of proteins according to their isoelectric point (p*I*) and mass [1]. Numerous articles have been dedicated to the high resolution of this technique [2–5]. A key point to get highly interpretable 2-DE maps is the solubilization of the biological sample [6, 7]. The first dimension, *i.e.*, isoelectric focusing (IEF), suffers from the interference with common substances, such as lipids, polysaccharides, and salts. Indeed, the high concentration of salt (>100 mM) within a sample solution (*e.g.*, physiological fluids) disturbs the electrophoresis process, by creating a high-conductivity zone in the immobilized pH gradient (IPG) gel [8]. A variety of sample clean-up techniques are used to circumvent this problem, such as, *e.g.*, dialysis [9], gel filtration [10], hollow fiber dialysis [11], and selective precipitation of proteins with dyes [12]. Furthermore, the sample, once separated by 2-DE and stained, requires new preparation steps before analysis by mass spectrometry (MS), which is known to be highly sensitive to the presence of salts and detergents. With the recent development of proteomics, extended efforts have been dedicated to the digestion of peptides or proteins and to desalting steps prior to MS, either by matrix-assisted laser desorption ionization-MS (MALDI-MS) or by electrospray ionization-MS (ESI-MS) [13–15]. Recently, new techniques have been proposed to improve the specific desalting process [14–23]. In 1987, Righetti *et al.* [24] showed that the use of a segmented IPG gel was an efficient manner to desalt and separate proteins in solution.

In 2002, we have shown that Off-Gel™ electrophoresis could be used to fractionate protein samples in solution without any ampholytes added. In Off-Gel™ electrophoresis, the biological sample to be purified is filled in a flow-chamber [25, 26] or in static multiwells [27], which are positioned on top of an IPG gel. The pH at the bottom of the chamber is chosen to be close to the p*I* of the proteins to be isolated. Two electrodes are placed at the extremities of the gel and when a direct current (DC) voltage is applied, the electric field penetrates into the flow-chamber causing the charged species to migrate from the chamber to the gel (*i.e.*, when $pH_{gel} < pI$ or $pH_{gel} > pI$). After fractionation, only globally neutral species (*i.e.*, $pI = pH_{gel}$) remain in the chamber. This technique allows an easy recovery of the purified compounds directly in solution. As for classical chromatographic methods, the advantage of Off-Gel™ electrophoresis is its ability to desalt during the separation step, which can avoid a specific desalting step.

Correspondence: Prof. Hubert H. Girault, Laboratoire d'Electrochimie Physique et Analytique, Ecole Polytechnique Fédérale de Lausanne, CH-1015 Lausanne, Switzerland
E-mail: Hubert.Girault@epfl.ch
Fax: +41-216933667

Abbreviations: AC, alternating current; **DC**, direct current

* Present address: Department of Analytical Chemistry, The Danish University of Pharmaceutical Sciences, DK-2100 Copenhagen, Denmark

In this paper, we report first the time evolution of the conductivity of a pure KCl or NaCl solution during Off-Gel™ electrophoresis. To follow the decrease of ionic strength, a conductometric cell with a large solution chamber was developed to implement additional measuring electrodes. A frequency response analyzer (FRA) was used to measure the impedance of the cell and to calculate the conductivity of the solution. The experimental data were analyzed using a simplified analytical model. As a proof of principle, a protein desalting experiment using the Off-Gel™ flow cell is then presented for a 0.1 M NaCl-β-lactoglobulin A solution. The analysis of the resulting sample is carried out by ESI-MS. Using the same geometry, a finite element diffusion migration model is used to show the effect of the electric field distribution in the cell on the desalting velocity.

2 Materials and methods

2.1 Chemicals

Sodium chloride (NaCl), potassium chloride (KCl), and acetic acid were purchased from Fluka (Buchs, Switzerland). Water of high resistivity (18.2 MΩ) was freshly prepared using a Milli-Q system from Millipore (Bedford, MA, USA). β-Lactoglobin A from bovine milk was purchased from Sigma (St. Louis, MO, USA). The protein stock solutions (1 mg·mL^{-1}) were prepared in pure water and used without further purification. IPG DryPlates (11 cm long linear pH gradient from pH 5 to 6) were purchased from Amersham Biosciences (Uppsala, Sweden). Methanol p.a. grade (99.9%) from Merck (Darmstadt, Germany) was used to prepare the spraying solution for the MS experiments.

2.2 Conductivity measurements

For the measurement of conductivity in the solution, the conductometric cell schematically depicted in Fig. 1a was used. The cell was assembled with a 4 × 4 cm^2 piece of an Immobiline gel placed between two plexiglass holders. The pH of the gel below the center of the chamber was equal to 5.1 as for the next section. Reservoirs and tubing were all filled with deionized water and the gel left to reswell for 30 min. Electrodes were carefully washed before any experiment and sonicated in pure water and in methanol to remove any contaminant. The open chamber was filled either with 2 mL KCl solution (10^{-4} M) or NaCl solutions ranging from 10^{-2} M to 10^{-3} M. A DC voltage of 100, 250, or 500 V (25, 62.5, 125 V·cm^{-1}, respectively) was applied through the gel. Impedance was measured using a frequency response analyzer Autolab PGSTAT 12

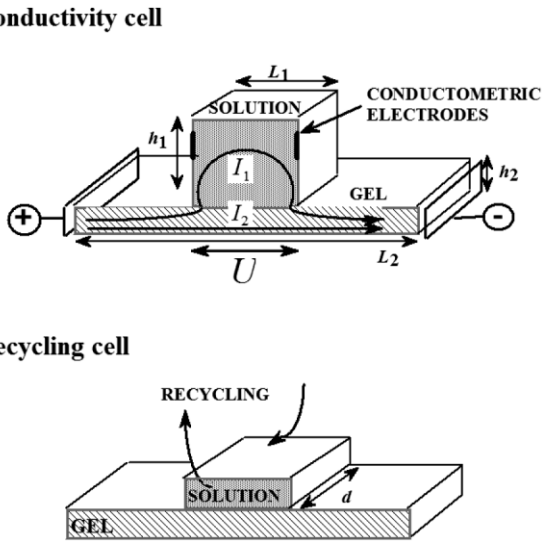

Figure 1. (a) Scheme of the current distribution within the solution (I_1) and the gel (I_2) in the conductometric cell. (b) Off-Gel™ cell employed for the desalting of a biological sample *via* a recycling pump. The set of dimension (h_1, L_1, h_2, L_2) are (10, 10, 1, 40 mm), (1, 4, 1, 40 mm) for geometry (a) and (b), respectively. In the geometry (b), the depth, d, is 20 mm leading to a chamber volume of 100 μL.

from Metrohm (Herisau, Switzerland). An alternating current (AC) potential of 0.1 V was applied at the two additional electrodes and the frequency decreased from 30 000 to 0.1 Hz. Impedance was then converted to conductivity for a given cell constant. Conductivity was also measured with a conductometer E 518 from Metrohm.

2.3 Desalting of a protein sample in the Off-Gel™ cell

To demonstrate the desalting capacity for protein samples, the cell presented in Fig. 1b was employed. The procedure, as described for the preparation of the gel, was used and a solution of β-lactoglobulin A (1 mg·mL^{-1}) in 0.1 M NaCl submitted to electrophoresis. The middle pH of the gel was chosen to fit with the p*I* of β-lactoglobulin A (*i.e.*, 5.1). The voltage was set at 100 V. The solution was recycled with the help of a peristaltic pump (Ismatec, Switzerland) at a rate of 50 μL·min^{-1}. After desalting of the solution, MS analysis was carried out on an ESI ion trap mass spectrometer LCQ Duo from Finnigan (San José, CA, USA) used in a positive ion mode. The samples were infused after dilution (1:10) in methanol:acetic acid:water (50:1:49 v/v/v) through a polyimide microchip (Diagnoswiss, Monthey, Switzerland) with a spray voltage of 2 kV [28]. Data acquisitions were performed in full-scan mode (*m/z* 150–2000).

2.4 Analytical model

In the Off-Gel™ principle, an electric field is applied across the gel (Fig. 1a) and some current lines pass through the solution above the gel. From an electrical point of view, this system can be modeled by two resistances in parallel, R_1 and R_2, representing the resistance in the solution and in the gel, respectively. The total current passing in the device can be simply described by

$$I_{tot} = I_1 + I_2 = U\left(\frac{1}{R_1} + \frac{1}{R_2}\right) \quad (1)$$

where I_1 is the current flowing through the solution, I_2 is the current passing through the gel, and U is the voltage applied at the edges of the chamber. Note that the pH in the IPG gel is fixed by a high concentration of Immobilines (10^{-2}–10^{-1} M). These amphoteric species, which are covalently linked to the acrylamide gel backbone, give a high buffering capacity to the fonctionalized gel.

In the chamber solution above the gel, cations and anions migrate towards the cathode and the anode, respectively (Fig. 2). To remove one mole of a (1:1) salt from the chamber, at least two coulombs are needed to address both the cations and the anions. The current, I_1, through the solution (Eq. 2) is therefore directly linked to the amount of ions transferred from the chamber to the solution of conductivity σ

$$I_1 = \frac{dq_1}{dt} = -\frac{2FVdc}{dt} = -\frac{2FVd\sigma}{\Lambda_m dt} \quad (2)$$

where q is the charge, F is the Faraday constant, V is the volume of the solution in the chamber, and Λ_m is the molar conductivity (assumed to be independent of the salt concentration under dilute conditions). On the basis of Table 1, the contribution of the proton migration to the current I_1 in solution is here neglected because of the higher concentration of salt compared to that of the protons (but staying in the dilute solution assumption, *i.e.*, ranging in the 10^{-4}–10^{-2} M range for a gel at pH 5). In that case, we can also assume that the resistance R_1 of the solution is not affected by the protons crossing the chamber but only depends on the conductivity of the electrolyte solution

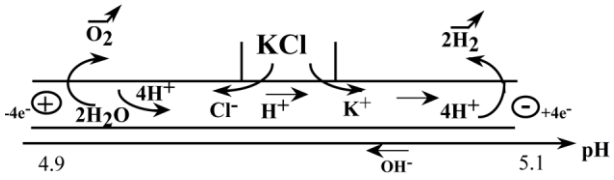

Figure 2. Schematic view of the ions' transport through the gel including the formation of hydrogen and oxygen at the respective cathodic and anodic electrodes, governed by the reduction and oxidation of water.

Table 1. Conductivity values (in $S \cdot m^{-1}$) of gels swollen in KCl solution (0.1 M) at different pH

	Pure solution	Gel medium		
–	–	pH 4.6 ± 0.1	pH 5.6 ± 0.1	pH 6.7 ± 0.3
KCl (0.1 M)	1.29	8.65×10^{-1}	7.21×10^{-1}	6.10×10^{-1}
Water	1.36×10^{-3}	4.74×10^{-3}	4.29×10^{-3}	3.67×10^{-3}

$$R_1 = \frac{k}{\sigma} \quad (3)$$

where k is the cell constant. It is worth noting that the charge balance of the solution is here considered in a global view (each K^+ going at one end being equilibrated by a Cl^- doing the same at the other end of the chamber). The local conservation of the electroneutrality condition, that induces electromigration dispersion (such as stacking effects) or diffusion potentials, will be taken into account in the numerical model. In the gel, the charge of the K^+ and Cl^- migrating fronts is assumed to be balanced by the concomitent supply of H^+ and OH^- from the electrodes ensuring the buffering capacity of the Immobilines.

Using Ohm's law ($I_1 = U/R_1$) to link Eqs. (2) and (3), we obtain the following differential equation, expressing the variation of the solution conductivity with time

$$\frac{2FVd\sigma}{\Lambda_m dt} + \frac{\sigma U}{k} = 0 \quad (4)$$

and taking as initial conditions $\sigma = \sigma_0$ the conductivity simply comes as

$$\sigma(t) = \sigma_0 \exp\left(-\frac{U\Lambda_m}{2FVk}t\right) \quad (5)$$

When a high concentration of salt (compared to the protons in the gel) has time to penetrate the gel before the application of the electric field, time is required to desalt the gel before the solution. Equation (5) becomes

$$\sigma(t) = \sigma_0 \exp\left(-\frac{U\Lambda_m}{2FVk}(t - t_d)\right) \quad (6)$$

where t_d is the desalting time of the gel. This two-resistance model can be completed by adding a resistance, R_3, for the lateral sides of the gel (see Addendum).

2.5 Numerical model

A previous model based on diffusion-equilibria equations had already been developed to study the influence of the buffering capacity of the gel at the solution/gel interface [26]. The present work studies the effects of the nonuniform conductivity distribution in the cell on the diffusion-

migration phenomena. Concerning electromigration phenomena, numerous mathematical and numerical studies have been presented in the literature, as for example [29–37], to describe the different modes of capillary electrophoresis or IEF processes. In a first approximation, the gel is considered as a supporting (*i.e.*, background) electrolyte, ensuring the initial current in the gel and the electroneutrality condition when the ions from the chamber (*i.e.*, K^+, Cl^-) are entering the gel. As a consequence, the acid-base reactions on the Immobilines and the physicochemical effects of the pH gradient are neglected.

As illustrated in Fig. 3, a four-species model was developed (from the two species one described in [38]). It consists of the (1:1) salt initially present in the solution (concentrations c_1, c_2) and of the (1:1) supporting electrolyte (concentrations c_3, c_4) assumed to be initially present in the entire domain to consider the buffering of the chamber by the gel. The electric field calculation is not decoupled from the transport Eq. (7), but is calculated simultaneously at each time step. To address this unknown (*i.e.*, ϕ), the electroneutrality equation (Eq. 8) is added to the transient diffusion-migration equation (Eq. 7) here expressed in the local form

$$\frac{\partial c_i}{\partial t} + \nabla \cdot \left(-D_i \nabla c_i - \frac{z_i F}{RT} D_i c_i \nabla \phi \right) = 0 \text{ for } i = 1,4 \qquad (7)$$

$$\sum_{i=1}^{4} z_i c_i = 0 \qquad (8)$$

where c_i, D_i, z_i, are respectively the concentration, the diffusion coefficient, and the electrical charge of the four species *i*. The last two properties are assumed to be uniform over the entire domain (z_{ci} = 1, −1, 1, −1, respectively, and $D_i = 1 \times 10^{-9}$ $m^2 \cdot s^{-1}$). As the model is not directly compared with the experiments, the diffusion coefficient was fixed at the order of magnitude of the considered salts NaCl and KCl. Moreover, the solution and gel are assumed to be convection-free and isothermal (natural convection neglected). No kinetic barriers are considered at the solution/gel interface as the gel could be considered as an aqueous solution [26].

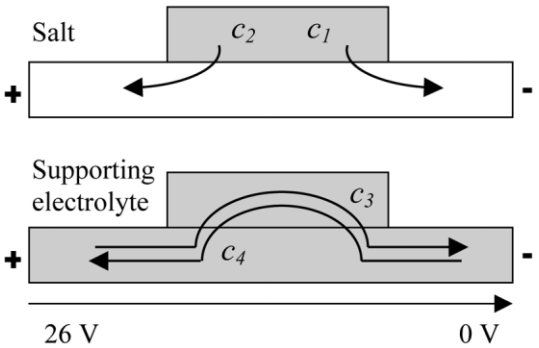

Figure 3. Scheme of the migration of the salt (c_1 and c_2) and of the supporting electrolyte (c_3 and c_4) in the cell where c_1 and c_2 are only present in the solution whereas c_3 and c_4 are arranged in the entire domain. The gel is 1 mm thick and 26 mm long with a potential difference of 26 V. The chamber dimensions are 1 × 4 mm.

The geometry used is a vertical cross-section of the device, consisting of solution and gel parts (transversal to the flow direction). It can be represented by a 2-D cross section of the cell (Fig. 1b) as the electrodes cover the entire lateral section of the gel. The size of the geometry is consistent with the dimensions of the experimental setup. The total gel length L_2 was fixed at 26 mm (ensuring that the migrating species do not reach the edges of the gel during the calculation time). A potential difference of 26 V was applied across the gel as boundary conditions (10 $V \cdot cm^{-1}$). The initial concentration of supporting electrolyte was fixed at 1 mM for all the calculations and the initial salt concentration in the chamber was varied (*i.e.*, 0.1, 0.5, 1, 2, 5 mM). The no flux conditions are imposed at all the boundaries of the domain excepted the extremities of the gel that are submitted to migration (c_3, c_4 = 1 mM is imposed at these extremities).

The 2-D cartesian model was implemented on the finite element commercial software Flux-Expert™ [39], operated on a Dell Linux PC (2 Gb RAM, 2.4 GHz frequency). The integral Galerkin formulation corresponding to Eqs. (7) and (8) is detailed in the Addendum. A nonlinear algorithm was used with a time step of 1 s (0.04% error compared to 0.5 s) and a precision convergence of 3% (less than 0.1% error compared to a 1% criteria). The mesh size, Δx, ranges from 30 μm (corner of the solution chamber) to 150 μm, ensuring a Courant-Friedrich-Levy number from 1.3 to 0.27, respectively (CFL = $v_m \cdot \Delta t/\Delta x$ where $v_m = \frac{zF}{RT} D \cdot \nabla \phi$ and Δt is the time step) and a maximum migration Peclet number ($Pe_m = v_m \cdot \Delta x/D$) ranging from 1.2 to 6.

3 Results and discussion

3.1 Conductivity measurements

The evolution of the desalting process was followed by conductivity measurements carried out using a diluted KCl electrolyte (*i.e.*, 1×10^{-4} M) as solution to desalt. Figure 4 presents the experimental time evolution of the solution conductivity (full lines and dots) for different voltages applied. The analytical results (dashed lines) are obtained with σ_0 taken as 1.49×10^{-3} $mol \cdot m^{-3}$, Λ_m as

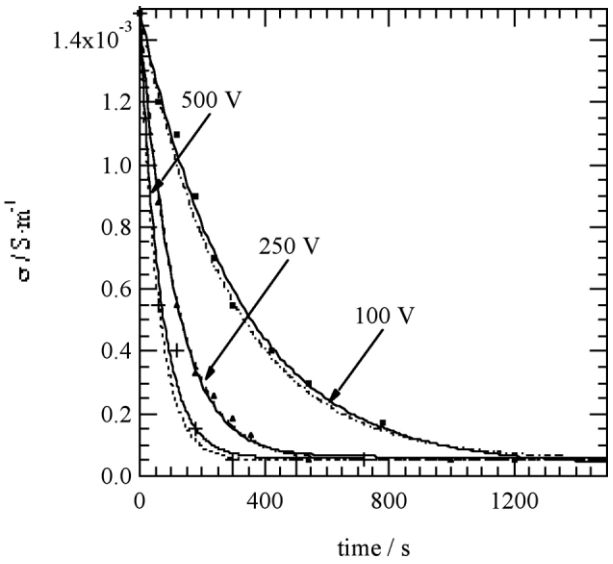

Figure 4. Effect of the applied voltage on the desalting of a 1×10^{-4} M KCl solution (geometry of Fig. 1a). Lines and markers represent the experimental data; dashed lines are the analytical results, taking σ_0 as 1.49×10^{-3} mol·m^{-3}, Λ_m as 1.49×10^{-2} S·m^2·mol^{-1}, V as 2×10^{-6} m^3, k as 222.4 m^{-1}, and U as 1/5 of the total voltage applied at the extremities of the gel. The baseline corresponds to the used deionized water conductivity.

1.49×10^{-2} S·m^2·mol^{-1} [40], V as 2×10^{-6} m^3, k as 222.4 m^{-1}. The cell constant, k, was obtained experimentally by measuring the cell resistance for KCl standard solutions of different concentrations. By fitting the calculation with the experimental results for a dilute solution, the voltage U on the solution chamber was found to be 1/5 of the total voltage U_{tot} applied on the cell. As a comparison, the theoretical value of the ratio U/U_{tot} is 1/7 when $R_1 = R_2$ (*i.e.*, $U = 0.5R_2 \cdot I$ and $U_{tot} = U + R_3 \cdot I = 3.5\ R_2 \cdot I$, where R_3 corresponds to the lateral parts of the gel whose total length is 30 mm compared to the 10 mm length of the chamber).

The conductivity of the solution was found to decrease exponentially, as predicted by Eq. (5) and a good agreement was obtained between the experimental and the calculated values for the different applied voltages. When the applied voltage increases, the time required to desalt the solution is reduced because of a higher migration velocity. With a voltage set at 500 V (*i.e.*, 125 V·cm^{-1}), the steady-state regime (corresponding to the complete sample desalting) is reached after 7 min (*i.e.*, 400 s) whereas for 100 V, 30 min (*i.e.*, 1800 s) are required. One can note that the desalting process is considered as terminated when the conductivity of the solution reaches the conductivity of the de-ionized water (measured before adding the salt at 0.5×10^{-4} S·m^{-1}).

To go towards more realistic conditions, higher salt concentrations (1×10^{-3} to 1×10^{-2} M NaCl) were used. For an imposed voltage of 100 V (25 V·cm^{-1}), the resulting conductivity was measured as a function of time, as shown in Fig. 5. Between the loading of the chamber and the establishment of the electric field, the salt has some time to diffuse into the gel (around 100 s). In that case, the main part of the current observed at the beginning of the experiment is used to desalt the gel below the chamber, which explains the plateau of conductivity observed in Fig. 5. This desalting delay is particularly important when the salt concentration is higher than the one of the proton in the gel, as illustrated by the increase of the plateau length with the concentration of salt. For the most concentrated solutions, the plateau length is then amplified by instrumental limitations. Indeed, the initial peak of current induced by the gel desalting is limited at the safety value imposed by the setup (10 mA) to avoid gel burning and gas evolution at the electrodes (see Fig. 2).

The time necessary to desalt the gel is illustrated by the curves (Fig. 5) which correspond to the fitting of the experimental results with the analytical model (Eq. 6). For the highest salt concentration (1×10^{-2} M), the plateau length is around 11 min (650 s) whereas it falls down to 2.5 min (150 s) for a concentration of 1×10^{-3} M. After this time, the usual exponential decrease is observed. Consequently, the complete desalting of the most concentrated solution requires 30 min (1800 s) while, for a 1×10^{-3} M solution, 18 min (1100 s) are necessary. These important desalting times can be explained by the big chamber size of the conductometric cell (10 mm height instead of 1 mm for the Off-gel™ recycling one).

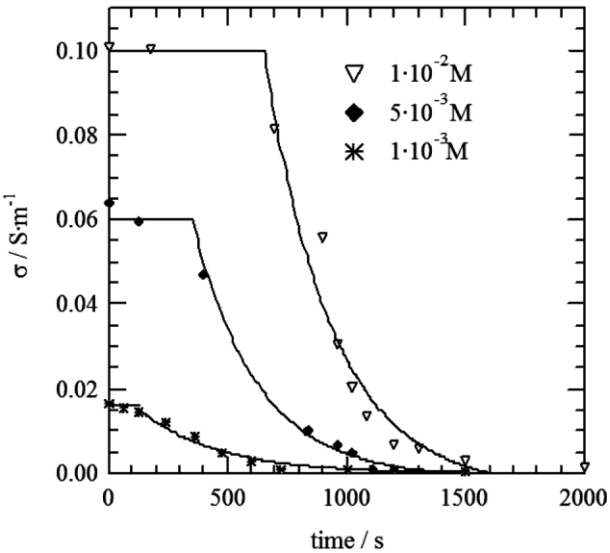

Figure 5. Conductivity evolution of NaCl solutions at different initial concentrations (1×10^{-2}, 5×10^{-3}, 1×10^{-3} M) during an Off-Gel™ run at 100 V (geometry of Fig. 1a).

3.2 Desalting of a protein solution in the Off-Gel™ cell

To illustrate the desalting principle of the Off-Gel™ flow cell, a solution of β-lactoglobulin A in 0.1 M NaCl was submitted to electrophoresis and the results visualized by ESI-MS (Fig. 6). The presence of salts in the sample can have many consequences, depending on their nature, their concentration, and on the settings of the ESI source used to transfer ions from the liquid phase to the gas phase (electrospray voltage, heated capillary voltage, and temperature in the case of the LCQ Duo used in this study with the microchip infusion). The main ones are (i) a decrease of sensitivity that has been the object of several fundamental studies [41–43], (ii) a peak-broadening that complicates mass assignment and spectrum deconvolution (see *e.g.*, [44]), and (iii) the apparition of salt clusters of the form $[M+nNa]^{n+}$. MS measurements were made before and after 1 h Off-Gel™ run (Fig. 6). Figure 6a shows the difficulty to analyze a spectrum with the presence of salt as explained in [22]. But after a 1 h run (Fig. 6b), the salt has efficiently been removed and the characteristic peaks of β-lactoglobulin A are well resolved.

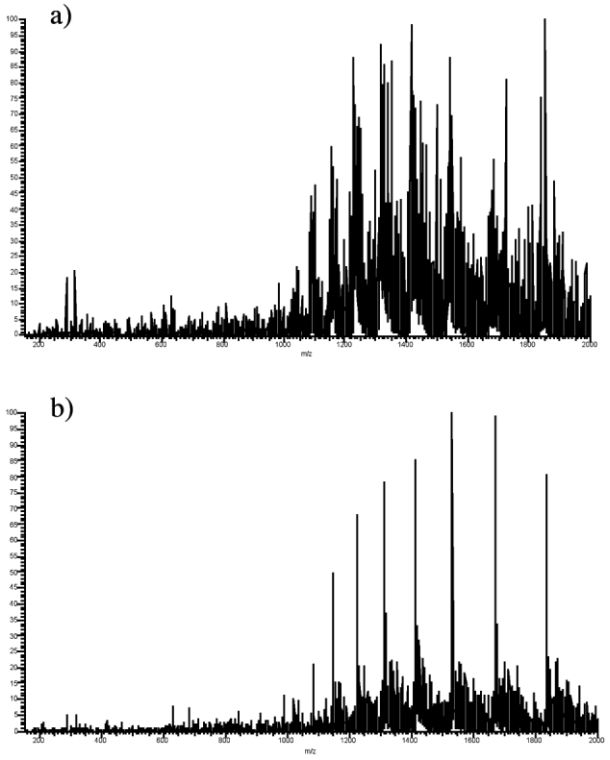

Figure 6. ESI-MS spectra obtained from a 1 $mg \cdot mL^{-1}$ solution of β-lactoglobulin A; (a) from the initial salty solution ([NaCl] = 0.1 M); (b) after 1 h desalting in the Off-Gel™ cell (Fig. 1b). The mixtures were diluted by a factor of 10 in a solution of methanol:acetic acid:water (50:1:49 v/v/v) before infusion.

3.3 Numerical simulation

The numerical model was used to illustrate the evolution of cations and anions coming from the electrolyte solution present in the chamber and migrating in the gel toward the anode and the cathode, respectively. When an electric field is applied along the IPG gel, the current lines pass through the flow chamber inducing the migration of the ions [25]. Figure 7a illustrates the concentration isovalues of the positive and negative ions after 60 s when the concentrations of salt and supporting electrolyte are identical ($c_{1,2}/c_{3,4} = 1$).

In the case of a solution that has a higher ionic strength than the gel, a greater fraction of the current lines pass through the chamber and should promote the ions migration. But the higher salt concentration also results in a local decrease of the electric field in the chamber (Fig. 8), reducing the local migration velocities of the ions following Eq. (7). This slowdown effect on the desalting process is shown in Fig. 7b representing isovalues of the salt anion concentration c_1, for two different concentration ratios (*i.e.*, $c_{1,2}/c_{3,4} = 1$ and 5) after a run of 200 s. As expected from the previous explanation, the higher the salt concentration ratio, the slower the removal of salt from the chamber.

4 Concluding remarks

In the present investigation, it is shown that Off-Gel™ electrophoresis can also be used to desalt a protein solution (in addition to its fractionation ability demonstrated previously). While remaining in solution, the sample can directly be involved in the next analysis step. Consequently, provided the realization of further developments, this technology could be downscaled to be envisaged as an on-line purification method integrating the desalting step. Using AC measurements, the evolution of the electrical conductivity of an electrolyte solution under Off-Gel™ electrophoresis was characterized. An analytical model was developed, showing a good agreement with the experiments. For the conductometric cell presently used (featuring a large chamber over gel height ratio) and high salt concentration, the beginning of the experiment is used to first desalt the gel. This situation is observed when the salts have time to diffuse in the gel before the application of the electric field. Going to the smaller geometry like the Off-Gel™ cell, a diffusion-migration finite element model was used, showing how the nonuniformity of the electric field through the cell (due to the salt) can slowdown the desalting process. To illustrate the desalting of a biological sample, a 1 $mg \cdot mL^{-1}$ solution of β-lactoglobulin A in 0.1 M NaCl was subjected to Off-Gel™ electrophoresis. The analysis of the resulting sample by ESI-MS demonstrates the effective removal of the salt.

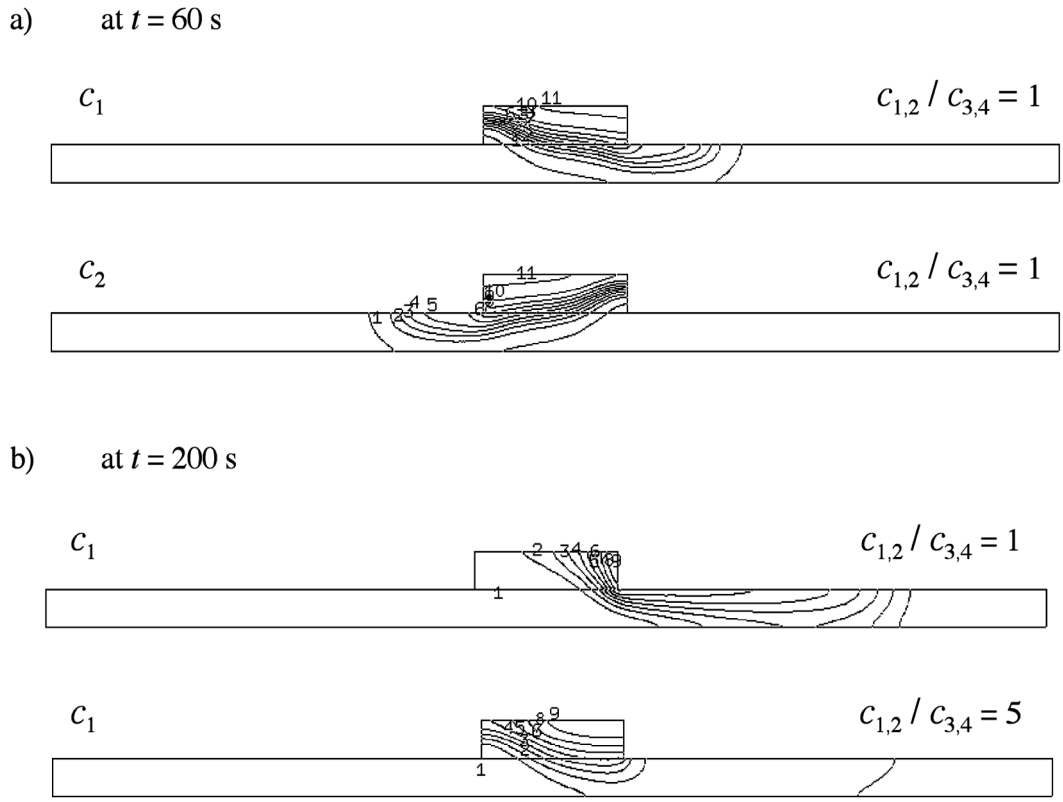

Figure 7. Concentration isovalues of (a) the anion, c_1, and the cation, c_2 after a 60 s run for a concentration ratio $c_{1,2}/c_{3,4}$ equal to 1, (b) c_1 after 200 s for $c_{1,2}/c_{3,4}$ equal to 1 and 5 (**grad**ϕ = 10 V·cm^{-1}). Lines 1, 2, 3, 4 .. represent respectively 1, 10, 20, 30..% of the maximum concentration (1 mM). The geometry and initial conditions are as in Fig. 3.

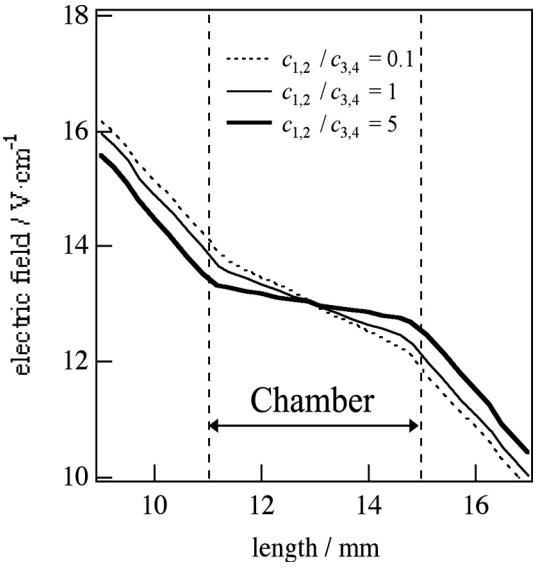

Figure 8. Electric field distributions along the gel/solution interface after a 60 s run. Three different salt over supporting salt concentration ratios are represented. The dashed lines show the limits of the chamber.

The authors wish to acknowledge the Fonds National pour la Recherche Scientifique Suisse for financial support.

Received November 3, 2004

5 References

[1] O'Farrell, P. H., *J. Biol. Chem.* 1975, *250*, 4007–4021.

[2] Pandey, A., Mann, M., *Nature* 2000, *405*, 837–846.

[3] Wilkins, M. R., Williams, K. L., Apple, R. D., Hochstrasser, D. F., *Proteome Research: New Frontiers in Functional Genomics*, Springer, Berlin 1997.

[4] Gorg, A., Obermaier, C., Boguth, G., Harder, A., Scheibe, B., Wildgruber, R., Weiss, W., *Electrophoresis* 2000, *21*, 1037–1053.

[5] Rabilloud, T., *Proteomics* 2002, *2*, 3–10.

[6] Rabilloud, T., *Electrophoresis* 1996, *17*, 813–829.

[7] Hochstrasser, D. F., Harrington, M. G., Hochstrasser, A. C., Miller, M. J., Merril, C. R., *Anal. Biochem.* 1988, *173*, 424–435.

[8] Strahler, J. R., Hanash, S. M., Somerlot, L., Bjellqvist, B., Görg, A., *Electrophoresis* 1988, *9*, 74–80.

[9] Manabe, T., Oda, O., Okuyama, T., *J. Chromatogr.* 1982, *241*, 361–370.

[10] Tragas, C., Pawliszyn, J., *Electrophoresis* 2000, *21*, 227–237.

[11] Zhang, R., Hjertén, S., *Anal. Chem.* 1997, *69*, 1585–1592.

[12] Marshall, T., Abbott, N. J., Fox, P., Williams, K. M., *Electrophoresis* 1995, *16*, 28–31.

[13] Larsen, M. R., Cordwell, S. J., Roepstorff, P., *Proteomics* 2002, *2*, 1277–1287.

[14] Liu, C. L., Hofstadler, S. A., Bresson, J. A., Udseth, H. R., Tsukuda, T., Smith, R. D., Snyder, A. P., *Anal. Chem.* 1998, *70*, 1797–1801.

[15] Jiang, Y., Hofstadler, S. A., *Anal. Biochem.* 2003, *316*, 50–57.

[16] Xu, N., Lin, Y., Hofstadler, S. A., Matson, D., Call, C. J., Smith, R. D., *Anal. Chem.* 1998, *70*, 3553–3556.

[17] Xiang, F., Lin, Y., Wen, J., Matson, D. W., Smith, R. D., *Anal. Chem.* 1999, *71*, 1485–1490.

[18] Ekstrom, S., Malmstrom, J., Wallman, L., Lofgren, M., Nilsson, J., Laurell, T., Marko-Varga, G., *Proteomics* 2002, *2*, 413–421.

[19] Jemere, A. B., Oleschuk, R. D., Ouchen, F., Fajuyigbe, F., Harrison, D. J., *Electrophoresis* 2002, *23*, 3537–3544.

[20] Tan, A. M., Benetton, S., Henion, J. D., *Anal. Chem.* 2003, *75*, 5504–5511.

[21] Yu, C., Davey, M. H., Svec, F., Frechet, J. M. J., *Anal. Chem.* 2001, *73*, 5088–5096.

[22] Lion, N., Gobry, V., Jensen, H., Rossier, J., Girault, H. H., *Electrophoresis* 2002, *23*, 3583–3588.

[23] Lion, N., Gellon, J. O., Jensen, H., Girault, H. H., *J. Chromatogr. A* 2003, *1003*, 11–19.

[24] Righetti, P. G., Barzaghi, B., Faupel, M., *J. Biochem. Biophys. Methods* 1987, *15*, 163–176.

[25] Ros, A., Faupel, M., Mees, H., van Oostrum, J., Ferrigno, R., Reymond, F., Michel, P., Rossier, J. S., Girault, H. H., *Proteomics* 2002, *2*, 151–156.

[26] Arnaud, I. L., Josserand, J., Rossier, J. S., Girault, H. H., *Electrophoresis* 2002, *23*, 3253–3261.

[27] Michel, P. E., Reymond, F., Arnaud, I. L., Josserand, J., Girault, H. H., Rossier, J. S., *Electrophoresis* 2003, *24*, 3–11.

[28] Gobry, V., van Oostrum, J., Martinelli, M., Rohner, T. C., Rossier, J. S., Girault, H. H., *Proteomics* 2002, *2*, 405–412.

[29] Mosher, R., Saville, D. A., Thormann, W., *The Dynamics of Electrophoresis*, VCH Publishers, Weinheim 1992.

[30] Foret, F., Křivánková, L., Boček, P., *Capillary Zone Electrophoresis*, VCH Publishers, Weinheim 1993.

[31] Beckers, J. L., Boček, P., *Electrophoresis* 2000, *21*, 2747–2767.

[32] Mao, Q. L., Pawliszyn, J., Thormann, W., *Anal. Chem.* 2000, *72*, 5493–5502.

[33] Mosher, R. A., Thormann, W., *Electrophoresis* 2002, *23*, 1803–1814.

[34] Beckers, J. L., Boček, P., *Electrophoresis* 2003, *24*, 518–535.

[35] Thormann, W., Huang, T., Pawliszyn, J., Mosher, R. A., *Electrophoresis* 2004, *25*, 324–337.

[36] Stedry, M., Jaros, M., Hruska, V., Gaš, B., *Electrophoresis* 2004, *25*, 3071–3079.

[37] Jaros, M., Hruska, V., Stedry, M., Zuskova, I., Gaš, B., *Electrophoresis* 2004, *25*, 3080–3085.

[38] Josserand, J., Lagger, G., Jensen, H., Ferrigno, R., Girault, H. H., *J Electroanal. Chem.* 2003, *546*, 1–13.

[39] Astek Rhône-Alpes, 1 place du Verseau, 38130 Echirolles, France, flux-expert@astek.fr.

[40] Atkins, P. W., *Physical Chemistry*, Oxford University Press, New York 1994.

[41] Constantopoulos, T. L., Jackson, G. S., Enke, C. G., *J. Am. Soc. Mass Spectrom.* 1999, *10*, 625–634.

[42] Enke, C. G., *Anal. Chem.* 1997, *69*, 4885–4893.

[43] Gamero-Castano, M., de la Mora, J. F., *Anal. Chim. Acta* 2000, *406*, 67–91.

[44] Benkestock, K., Edlund, P. O., Roeraade, J., *Rapid Commun. Mass Spectrom.* 2002, *16*, 2054–2059.

6 Addendum

6.1 Extended analytical model

The Off-Gel™ system can be represented by a set of three resistances as shown below, where U_{tot} is the total voltage passing through the three resistance system.

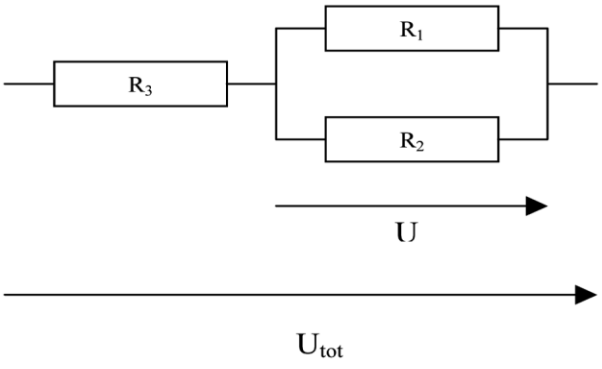

By applying Ohm's law for *U*, it is written

$$U = R_1 I_1 = \frac{k_1}{\sigma + \sigma_h} I_1 \quad \text{(A.1)}$$

$$\text{and } U = R_2 I_2 = \frac{k_2}{\sigma + \sigma_g} I_2 \quad \text{(A.2)}$$

where σ_g and k_2 are the conductivity and the cell constant of the gel, respectively.

Rearrangement gives

$$I_2 = I_1 \left(\frac{k_1}{\sigma + \sigma_h}\right)\left(\frac{\sigma + \sigma_g}{k_2}\right) \quad \text{(A.3)}$$

Using Eq. (A.1–3), U_{tot} is expressed as

$$U_{tot} = \left(R_3 + \frac{1}{\frac{1}{R_1} + \frac{1}{R_2}}\right)(I_1 + I_2)$$

If $R_3 = xR_2$, then:

$$= \left[\frac{xk_2}{\sigma + \sigma_g} + \frac{1}{\frac{\sigma+\sigma_h}{k1} + \frac{\sigma+\sigma_g}{k_2}}\right] \cdot I_1 \left[1 + \left(\frac{k_1}{\sigma + \sigma_h}\right)\left(\frac{\sigma + \sigma_g}{k_2}\right)\right] \quad \text{(A.4)}$$

Inserting Eq. (3) into Eq. (A.4), it is obtained

$$U_{tot}dt = \left[\frac{xk_2}{\sigma+\sigma_g} + \frac{1}{\frac{\sigma+\sigma_h}{k1} + \frac{\sigma+\sigma_g}{k_2}}\right] \left[1 + \left(\frac{k_1(\sigma+\sigma_g)}{k_2(\sigma+\sigma_h)}\right)\right]\left[\frac{-FV}{2\Lambda_m}\right]d\sigma \quad (A.5)$$

Rearrangements give

$$U_{tot}dt = \left[\frac{(1+x)k_1}{\sigma+\sigma_h} + \frac{xk_2}{\sigma+\sigma_g}\right] \cdot \left[\frac{-FV}{2\Lambda_m}\right]d\sigma \quad (A.6)$$

Taking at $t = 0$, $\sigma = \sigma_0$, Eq. (A.6) becomes

$$-\frac{2U_{tot}\Lambda_m}{FV}t = \ln\left[\left(\frac{\sigma+\sigma_h}{\sigma_0+\sigma_h}\right)^{(1+x)k_1}\left(\frac{\sigma+\sigma_g}{\sigma_0+\sigma_g}\right)^{xk_2}\right] \quad (A.7)$$

Taking $x = 0$, *i.e.*, neglecting the gel resistance outside of the focusing zone, Eq. (A.7) becomes:

$$-\frac{2U_{tot}\Lambda_m}{FV}t = \ln\left(\frac{\sigma+\sigma_h}{\sigma_0+\sigma_h}\right)^{k_1} \quad (A.8)$$

The expression is there similar to Eq. (5)

$$(\sigma+\sigma_h)_t = (\sigma_0+\sigma_h)\ \exp\left(-\frac{U_{tot}\Lambda_m}{2FVk1}t\right) \quad (A.9)$$

with $U = U_{tot}$

6.2 Numerical formulation of the model

Equations (7) and (8) are derived in the global general form (A.10) and (A.11), using the Galerkin's formulation, frequently used in the finite element method (multiplication by a projective function α and integration on the domain of study, *W*).

$$\iint_W \alpha\left[\frac{\partial c_i}{\partial t} + \nabla\cdot\left(-D_i\nabla c_i - \frac{z_iF}{RT}D_ic_i\nabla\phi\right)\right]dW = 0 \quad (A.10)$$

$$\iint_W \alpha\sum_{i=1}^{4}[z_ic_i]\ dW = 0 \quad (A.11)$$

where i = 1–4.

By decomposing the product between α and the divergence, the second order derivative of (A.10) (divergence of the gradient) is turned as follows:

$$\alpha\ \nabla\cdot(-D_i\nabla c_i) = \nabla\cdot(-\alpha D_i\nabla c_i) + D_i\ \nabla\alpha\cdot\nabla c_i \quad (A.12)$$

Injecting (A.12) in (A.10) and using the Ostrogradsky theorem, the divergence term is rejected at the boundary, where it expresses the flux conditions of the species. In the present case of study, this boundary condition equals to zero (no flux at the boundaries of the domain).

$$\iint_W \left[\alpha\frac{\partial c_i}{\partial t} + D_i\nabla\alpha\cdot\nabla c_i + \frac{z_iF}{RT}D_i\,c_i\nabla\alpha\cdot\nabla\phi\right]dW = 0 \quad (A.13)$$

Applying (A.12) to (A.10), and writing the initial system (A.10, 11) in a matricial and local form for the four species, we obtain (A.14), where β is the interpolation function of the unknown vector [c_1, c_2, c_3, c_4, ϕ]. All the gradients are written in the nabla form ∇.

$$\begin{bmatrix}\alpha&0&0&0&0\\0&\alpha&0&0&0\\0&0&\alpha&0&0\\0&0&0&\alpha&0\\0&0&0&0&0\end{bmatrix}\cdot\begin{bmatrix}\frac{\partial c_1}{\partial t}\\\frac{\partial c_2}{\partial t}\\\frac{\partial c_3}{\partial t}\\\frac{\partial c_4}{\partial t}\\\frac{\partial\phi}{\partial t}\end{bmatrix} + \begin{bmatrix}D_1\nabla\alpha\nabla\beta&0&0&0&\frac{z_1F}{RT}D_1c_1\nabla\alpha\nabla\beta\\0&D_2\nabla\alpha\nabla\beta&0&0&\frac{z_2F}{RT}D_2c_2\nabla\alpha\nabla\beta\\0&0&D_3\nabla\alpha\nabla\beta&0&\frac{z_3F}{RT}D_3c_3\nabla\alpha\nabla\beta\\0&0&0&D_4\nabla\alpha\nabla\beta&\frac{z_4F}{RT}D_4c_4\nabla\alpha\nabla\beta\\\alpha z_1\beta&\alpha z_2\beta&\alpha z_3\beta&\alpha z_4\beta&0\end{bmatrix}\cdot\begin{bmatrix}c_1\\c_2\\c_3\\c_4\\\phi\end{bmatrix} = 0 \quad (A.14)$$